Experiment and theory for the reaction ^{7}Li$(\gamma,t)^4$He for $E_\gamma < 50$ MeV

D. M. Skopik, J. Asai, E. L. Tomusiak, and J. J. Murphy II
Saskatchewan Accelerator Laboratory, University of Saskatchewan, Saskatoon, S7N 0W0, Canada
(Received 23 July 1979)

Differential and total cross sections for the ^{7}Li$(\gamma,t)^4$He reaction were measured. Both real and virtual photons were used in the experiment and gave self-consistent results. The data show a broad resonance indicating the presence of positive parity states near 8 MeV excitation in ^{7}Li. A calculation using an α-^{3}H cluster model of ^{7}Li was also performed. Poor agreement is found between the calculation and experimental results.

[NUCLEAR REACTIONS ^{7}Li$(\gamma,t)^4$He, measured $\sigma(E;E_\alpha,\theta_\alpha)$ and $(E;E_t,\theta_t)$ calculated ^{3}H-α cluster model cross section.]

I. INTRODUCTION

In an earlier paper,[1] we reported on the ^{7}Li$(\gamma,t)^4$He cross section at 90° and noted large discrepancies in the previously published data over the energy range $E_x = 5$ to 20 MeV. Earlier experiments show a large number of peaks, and the magnitudes of the published cross sections vary by up to two orders of magnitude. This work is an extension of our earlier paper whereby we have extended the maximum excitation energy to 50 MeV and have performed an angular distribution over the excitation interval of 5 to 15 MeV. The aim of the experiment is essentially twofold. First, the existence of a broad positive parity resonance(s) having $J^\pi = \frac{1}{2}^+, \frac{3}{2}^+$ has been postulated to explain the nature of the cross section for the reaction ^{6}Li$(n,\alpha)^3$H at low energies.[2] Since these states would most likely involve $E1$ absorption, the $\alpha + T$ channel should be well suited to determine if a resonance does exist. Secondly, by measuring an angular distribution in this energy region we hope to ascertain if any of the known negative parity $T = \frac{1}{2}$ states that have been established[3] are reflected in this channel. These negative parity states would be difficult to see in a yield curve, but should be manifested through interference, by an asymmetry in the angular distribution.

The bulk of the photodisintegration data reported here is derived from the ^{7}Li$(e,t)^4$He$,e'$ reaction using plane wave virtual photon analysis (VPA), since distortion effects for a light nucleus such as ^{7}Li are negligible. To check the accuracy of the VPA, we have also taken a number of runs with different thicknesses of Ta radiators in front of the target to determine the real photon cross section in the region where VPA is least trustworthy, namely, for excitation energies much less than the incident electron beam energy.

II. EXPERIMENTAL PROCEDURES AND ANALYSIS

This experiment was performed using the positive ion spectrometer facility of the Saskatchewan electron linear accelerator laboratory. Since this facility has been described in detail in other papers,[4,5] only a brief description will be given here.

The momentum analyzed electron beam was incident on a self-supporting target foil of natural lithium (92.4% ^{7}Li, 7.6% ^{6}Li). The target was obtained by rolling lithium to the desired thickness. To prevent oxidation the target was kept in mineral oil during fabrication and until it was placed in the scattering chamber, at which time it was cleaned with trichloroethylene, which in turn was then pumped off the surface of the Li foil in the scattering chamber. This procedure eliminates problems with ^{12}C, ^{15}N, and ^{16}O contaminants which could be present during the fabrication procedure.

The target thickness was determined by direct measurement with a micrometer. The uniformity of target thickness was checked by comparing yields from different parts of the target. No differences in thickness were observed at the 5% level. In addition several Li foils were prepared ranging in thickness from 2–4 mg/cm^2. Triton and alpha yields from these different targets agreed to within 10%.

To guard against target melting which would change the target thickness, the electron beam current was limited to ≤ 10 μA; furthermore, at each incident electron energy and spectrometer angle the first and last runs were made at the same spectrometer magnetic field setting. Comparison of yields for these pairs of runs indicates that there was no change in target thickness during any set of runs. As a final check, a comparison of

yields from the first runs of the experiment with yields from the final runs was made. Both sets of yields were for the same incident electron energy and spectrometer settings. Again no evidence of a change in target thickness was found.

The tritons and alpha particles were detected and identified by a magnetic spectrometer. This spectrometer consists of five silicon surface barrier detectors positioned in the focal plane of a 127° double-focusing magnet. The spectrometer is coupled to the scattering chamber by a sliding seal that permits measurements at any angle between 27° and 152° from the beam line. The energy calibration, energy acceptance, and solid angle of the spectrometer were determined by the use of 5.49 MeV α particles from an ^{241}Am source. The incident beam current was measured by a SLAC-type nonintercepting ferrite monitor whose response was checked against a Faraday cup and was found to be linear and reproducible to better than 2%. The total error associated with solid angle, energy acceptance, number of target nuclei, and incident electron flux is $\leq 15\%$, which is primarily due to the problems associated with fabrication of the Li foils.

To ensure that detected particles originated in two-body disintegrations it was necessary to restrict excitation energies to within 6.3 (19.8) MeV of the incident electron energy when ^{4}He's (^{3}H's) were detected. Therefore, yields were obtained for incident electron energies of 20.5, 25, 30, 35, 40, 45, and 50 MeV. The incident electron energy is determined and measured by a slit and magnet beam handling system which has been calibrated by elastic electron scattering at a variety of energies. During this experiment the slits were set to allow an energy spread of ±1%.

The triton angular distribution data were taken with an incident beam energy $E_0 = 25.0$ MeV. Note that for $E_\gamma \lesssim 10.6$ MeV tritons could arise from the small ^{6}Li impurity in the target. To determine if this effect was significant the 90° cross section was measured at $E_0 = 20.5$ MeV, which kinematically eliminates any tritons from the ^{6}Li(e,t) reaction ($Q = 15.791$ MeV). Within the statistical accuracy of the experiment (2–3%) no differences were observed for these two incident electron energies. Hence the cross sections for $E_0 = 25$ MeV are taken to be solely from the ^{7}Li(e,t) reaction, and the ^{6}Li(e,t) yield is negligible for our range of kinematic parameters.

Furthermore, the process of insuring only two-body breakup when the alpha particles were measured (i.e., measuring the cross section at an excitation energy within 6.3 MeV of the incident electron energy) eliminates, due to much higher thresholds, any possibility of contaminants such as ^{12}C, ^{15}N, and ^{16}O contributing to the alpha particle cross sections.

The pulse height spectra for the five detectors were accumulated in five 256-channel analog to digital converters (ADC) interfaced to a PDP 11-55 computer through CAMAC. The ADC's were gated by the accelerator master trigger for 2 μs at each beam burst. Since the energy deposited in each detector at a particular magnetic field setting is proportional to Z^2/M of the various particles incident on the detectors, protons and α particles would produce a single peak in each pulse height spectrum. However, since the α particles stop after passing through much less material than that required to stop the protons and since the sensitive depth of our detectors can be reduced by lowering the applied bias voltage, by a judicious choice of bias voltage it is possible to recover the full α-particle signal while obtaining only a small fraction of the proton signal, thus separating the α-particle and proton peaks in the pulse height spectra.

The peaks of interest in each spectrum were integrated to obtain the number of particles detected. When required, a background, obtained by least-squares fitting a smooth curve to points above and below the peak, was subtracted before the integration was performed. These yields are used to calculate first an electrodisintegration cross section. From this cross section a photodisintegration cross section is obtained using virtual-photon theory. The electrodisintegration cross section at a spectrometer angle θ and for a particle energy E is given by

$$\frac{d^2\sigma}{d\Omega dE} = \frac{C(\theta,E')}{\Delta\Omega \Delta E' n_t(\theta)} \frac{\Delta E'}{\Delta E} ,$$

where $C(\theta,E')$ is the number of particles detected per incident electron, $\Delta\Omega$ is the spectrometer solid angle, $n_t(\theta)$ is the number of target nuclei per unit area, E' is the energy of the detected particle, $\Delta E'$ is the energy acceptance of the spectrometer, and ΔE is the corresponding energy bite at the center of the target. E was calculated from E' using the Bethe-Bloch formula and assuming the detected particle originated halfway through the target foil. The two energy bites ΔE and $\Delta E'$ are related by (assuming $dE/dx \sim 1/E$):

$$\frac{\Delta E'}{\Delta E} = \left(\frac{dE}{dx}\right)_f \Big/ \left(\frac{dE}{dx}\right)_i .$$

The subscripts f and i indicate that the energy loss per unit length is to be evaluated at the kinetic energy of the detected particle at the spectrometer (f) and at the center of the target (i).

The details of virtual photon analysis of electrodisintegration data are given in Ref. 5. In brief,

if a single multipolarity dominates, the photodisintegration cross section is given by

$$\frac{d\sigma}{d\Omega}=\frac{d^2\sigma}{d\Omega dE}\,\frac{1}{[N(E_0,E_\gamma)/E_\gamma]}\,\frac{dE}{dE_\gamma}\,, \tag{1}$$

where E_γ is the photon energy calculated with photon kinematics, $N(E_0,E_\gamma)$ is the number of virtual photons of energy E_γ for an incident electron energy of E_0, and dE/dE_γ is obtained from the expression for E_γ:

$$E_\gamma=\frac{m_t E+Q(m_t-m_p+Q/2)}{m_t-m_p-E+p_p\cos\theta}\,.$$

The target mass is m_t, m_p is the detected particle mass, Q is the photodisintegration reaction threshold, and p_p is the detected particle momentum; E and θ were defined earlier. The quantity $N(E_0,E_\gamma)$ in Eq. (1) is multipole dependent. However, the data analysis is straightforward if one multipole is dominant or if the data are taken near the "tip" of the virtual-photon spectrum. This latter case is illustrated in Fig. 1 which shows the number of virtual photons for various multipoles.

The angular distribution data were analyzed two ways. First, the photo cross sections were formed by using in Eq. (1) the expression

$$N(E_0,E_\gamma)=\frac{\alpha}{\pi}\,\frac{\{R_E^2+[(1+R_E^2)\lambda-2R_E-\frac{3}{2}R_E^2]\sin^2\theta\}}{\sin^2\theta}\,, \tag{2}$$

where

$$R_E=(E_0-E_\gamma)/E_0\,,$$
$$\lambda=\ln\frac{2E_0(E_0-E_\gamma)}{m_e E_\gamma}\,. \tag{3}$$

These cross sections were then least-squares fitted to the expression

$$\sigma(\theta)=\sum_{l=0}^{4}C_l P_l(\cos\theta)\,. \tag{4}$$

The coefficient C_4 which arises from $E2$ transitions was found to be non-negligible. Since the number of $E2$ virtual photons is greater than the number of $E1$ virtual photons, the analysis was also performed by taking into account the dependence of the virtual-photon spectrum upon the multipolarity using the expressions in Ref. 5 which includes $E1$, $E2$, and $M1$ multipoles. It was found that the only significant change was for $E_\gamma \lesssim 12$ MeV where the magnitude of the cross section is lower by $\approx 15\%$ from that obtained when Eq. (2) was used in the analysis. The fact that we have used a virtual-photon theory where the initial state consists of two nuclear fragments having relative angular momentum $l=0$ is not expected to significantly alter the analysis. An arbitrary initial state in the virtual-photon theory, the real tially makes the cross section more isotropic.[6] We find that the isotropic component in the angular distribution is zero within the experimental error over the energy region where a significant difference was found between the two analysis methods.

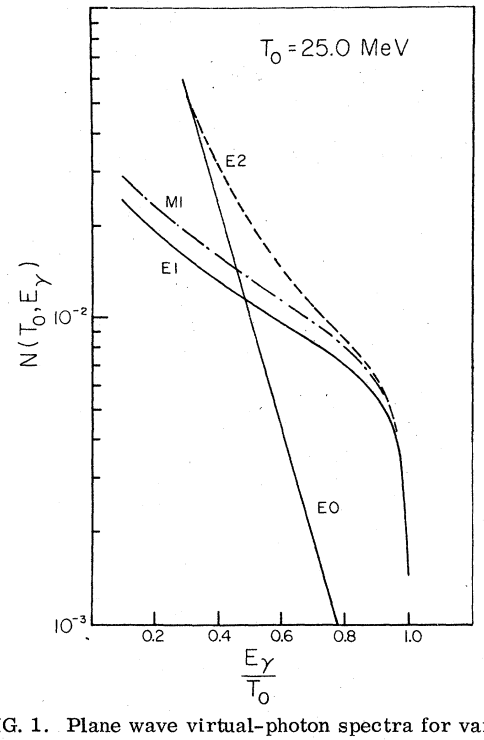

FIG. 1. Plane wave virtual-photon spectra for various multipoles. The large $E2$ spectrum indicates that if $E2$ transitions are contributing significantly [as reflected in the $l=4$ Legendre coefficient of Eq. (4)], the extracted photo data will be lower from what are obtained using only an $E1$ spectrum. Our radiator measurements indicate that $E\emptyset$ transitions do not contribute significantly to this breakup mode and are not included in the analysis.

As a check on the virtual-photon theory, the real photon cross section was measured by inserting thin (10.6–42.4 mg/cm^2) Ta radiators in front of the ^{7}Li foil. Radiator in and radiator out runs were made and the real photo cross section was found using formula 3BSe given in Koch and Motz.[7] Runs with an empty target holder were also made to insure that tritons from the Ta foil were not entering the spectrometer. The results of these measurements near the low energy peak of the cross section at $E_\gamma=7.75$ MeV are

$$\frac{\sigma(\text{virtual photon analysis})}{\sigma(\text{real photon analysis})}=1.02\pm0.09\,.$$

Thus the virtual-photon analysis is valid to within 9% in this experiment.

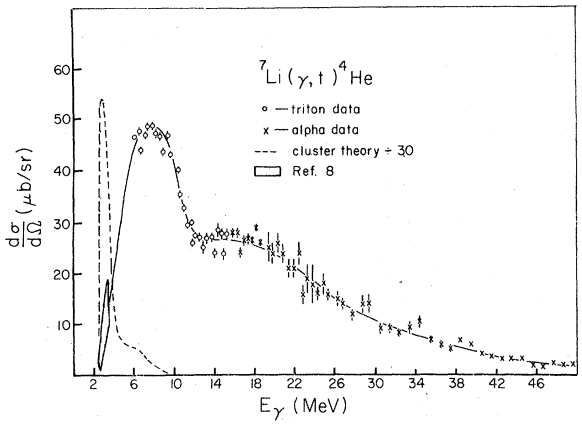

FIG. 2. The 90° cross section for the (γ, t) and (γ, α) reactions. The ^{7}Li$(\gamma, t)^4$He measurement is indicated by the open circles, while the ^{7}Li$(\gamma, \alpha)^3$H measurement is indicated by the crosses. The dashed line is the result of the theory described in the text. The solid line is only meant to guide the eye.

III. RESULTS

The 90° differential cross section

The 90° photodisintegration cross section for the α-^{3}H breakup of ^{7}Li is shown in Fig. 2. For $E_x \gtrsim 14.5$ MeV, α particles were measured, since the magnetic spectrometer limits the maximum triton energy to approximately 7 MeV. Also shown in Fig. 2 is the capture data of Griffiths *et al.*[8] Detailed balance has been used to convert their data to photodisintegration cross sections. While the capture experiment was performed over a very limited energy region, the rise of the cross section after threshold appears to be consistent with the lowest points measured in our experiment.

These data indicate that a broad resonance (most probably $E1$ in nature) exists at approximately 7 MeV excitation in ^{7}Li, having a width of ≈7 MeV. The J of this resonance cannot be uniquely assigned, but the angular distribution data are consistent with a positive parity resonance having possible J^π values of $\frac{1}{2}^+$, $\frac{3}{2}^+$, $\frac{5}{2}^+$ (or mixtures thereof).

In addition there is slight evidence of a smaller but very broad state around $E_x = 18$ MeV, with the cross section at higher energies decreasing smoothly with increasing photon energy.

We note that a discrepancy exists in the absolute magnitude of our 90° cross section and that measured at Giessen[9] (our data are higher). While our earlier work[1] which was measured at only one angle should be renormalized by a factor of 0.85 to take into account the presence of $E2$ virtual photons, as mentioned in the previous section, the disagreement still persists and amounts to a factor of 1.2. Since the virtual-photon-extracted data are consistent with our real photon measurements, the difference is not due to the use of VPA but is probably related to problems connected with fabrication of the Li targets.

Angular distribution measurements

We have measured the angular dependence of tritons over an excitation range of 6 to 15 MeV in ^{7}Li. These data were taken at seven laboratory angles in 200 keV steps. As mentioned above, the data were fitted to a Legendre expansion and the quantities $4\pi C_0$ and C_1/C_0 are shown in Figs. 3 to 5. The odd terms in the Legendre fit arise from interference of transition matrix elements having different parity and are most likely due to interference between $E1$ and $E2$ terms. As noted in the introduction, several $T=\frac{1}{2}$ natural parity states have been observed in ^{7}Li, and it might be expected that these states would appear in the angular distribution through interference effects.

The coefficients C_1/C_0 and C_3/C_0 are shown in Fig. 4. Several changes in sign of C_3/C_0 are apparent, the first two occurring near the locations of the $\frac{5}{2}^-$, $T=\frac{1}{2}$ states at 6.68 and 7.47 MeV. Both C_1/C_0 and C_3/C_0 change sign at $E_x \approx 11$ MeV. However, the only reported level at this excitation energy in ^{7}Li has been assigned $T=\frac{3}{2}$ which, if pure $T=\frac{3}{2}$, could not appear in this channel.

The other most notable feature of the angular distribution data is the presence of a significant

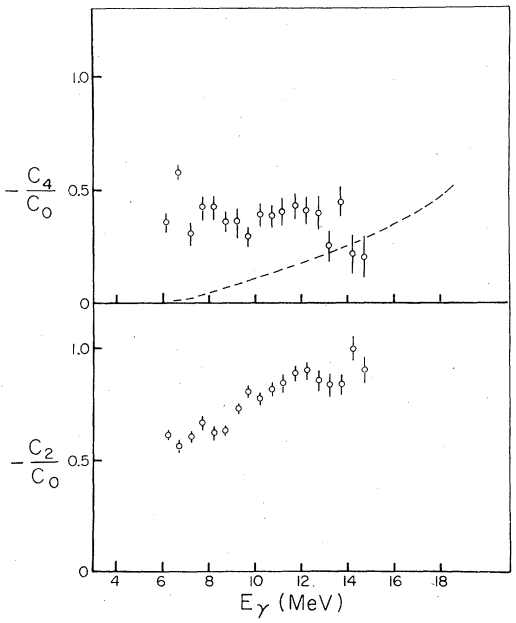

FIG. 3. Even Legendre coefficients found by least-squares fitting the data to Eq. (4). The dashed line indicates the $E2$ strength in our α-^{3}H cluster model.

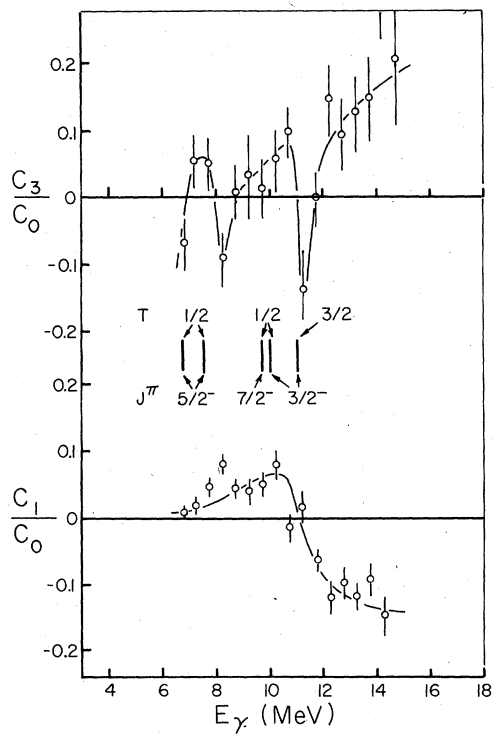

FIG. 4. Odd Legendre coefficients. The location of the known negative parity states in ^{7}Li are indicated.

value of C_4/C_0, indicating the presence of appreciable $E2$ absorption. Again, since interference between a number of $E2$ transition matrix elements may result in a finite value of C_4/C_0, little can be said concerning the specific transition matrix element(s) involved.

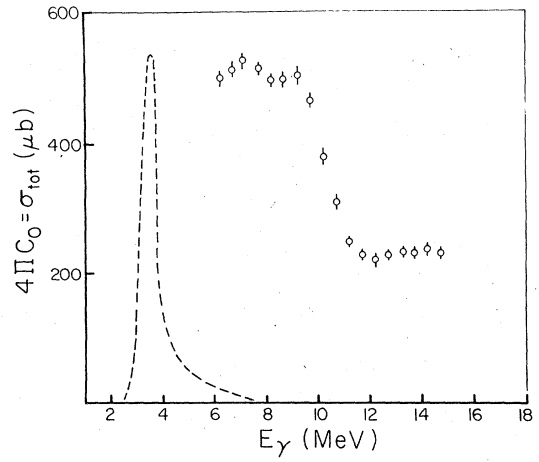

FIG. 5. The total cross section determined from the angular distribution data. The dashed line is the theory divided by 30.

Total cross section

The total cross section can be determined from the angular distribution data and is given by $4\pi C_0$. These data are shown in Fig. 5 and exhibit the same resonance shape as was noted in the 90° cross section. The maximum excitation energy in this case, however, is limited by the ability of the spectrometer to bend only tritons with $E_t \lesssim 7$ MeV. If we use these data together with the 90° data shown in Fig. 2, we find that the (γ,t) cross section integrated from threshold to 50 MeV gives 8.1 MeV mb; in other words ≈50% of the (γ,n) or (γ,p) integrated cross section. We have also fitted the low energy peak with Lorentz and Breit-Wigner line shapes. The fits were similar with the Breit-Wigner line shape giving a slightly better χ^2. The integrated cross section for the low energy resonance was found to be 6.2 MeV mb, hence 77% of the integrated cross section for this channel is located in the low energy resonance, which from the Breit-Wigner fit was found to have $\Gamma = 7.2$ MeV centered at $E_R = 7.7$ MeV.

IV. THEORY

It is instructive to compare our measured cross sections with those calculated using a simple model. The nature of the reaction considered here suggests that an α-^{3}H cluster model be considered. In this picture there are two particles, a triton and an alpha particle, which interact via an assumed two-body potential. The alpha and triton are given form factors, but other than this they are assumed to be structureless. A remnant of the Pauli principle between nucleons appears now as a restriction on the wave function which describes the relative motion of the α-^{3}H pair in the ground state. In detail, this wave function must be a $1P$ function (i.e., one node with $l=1$) so that we write for the ground state

$$|J=\tfrac{3}{2}M\rangle = |\alpha\rangle[\,|T;j=\tfrac{1}{2}\rangle \otimes \phi_{11}(\vec{r})]_M^{3/2}\,,$$

where $\phi_{nlm}(\vec{r}) = R_{nl}(r)Y_{lm}$ is the relative motion wave function and the α and triton vectors are written in a standard notation. The final state which corresponds asymptotically to relative motion of energy $\hbar^2K^2/2\mu$ in a Coulomb field $2e^2/r$ is written as

$$|\vec{K},\sigma\rangle = |\alpha\rangle \frac{4\pi}{\sqrt{8\pi^3}} \sum_{lm} i^l R_l(Kr)Y_{lm}(\hat{r})Y^*_{lm}(\hat{K})\,|T;\tfrac{1}{2}\sigma\rangle\,,$$

where

$$R_l(Kr) \sim \frac{1}{Kr}\,[\cos\delta_l F_l(Kr) + \sin\delta_l G_l(Kr)]\,.$$

To determine the bound state wave function R_{11} and the continuum $R_l(Kr)$ we need to specify an α-^{3}H potential. We have used the Woods-Saxon

model

$$V(r) = V_0[1 + e^{(r-R_0)/t}]^{-1} + V_c ,$$

where

$$V_0 = -52 \text{ MeV} ,$$

$$R_0 = 2.5 \text{ fm}, \quad t = 1.5 \text{ fm} ,$$

and

$$V_c = 0.72(3 - \tfrac{1}{4}r^2) \text{ MeV}, \quad r \leq 2 \text{ fm}$$

$$= 2.88/r \text{ MeV}, \quad r \geq 2 \text{ fm}.$$

These parameters bind the $n=1$ $l=1$ level by 2.45 MeV (the α-^{3}H separation energy is 2.47 MeV) and give a charge radius of 3.03 fm as compared to a measured charge radius of 2.37 fm. In the cluster model of ^{7}Li the charge radius is determined by

$$\langle r^2 \rangle_{^7\text{Li}} = \tfrac{2}{3}\langle r^2 \rangle_\alpha + \tfrac{1}{3}\langle r^2 \rangle_T + \tfrac{34}{147} \int_0^\infty (R_{11})^2 r^4 dr .$$

Finally the photodisintegration cross section including only $E1$ and $E2$ multipoles is given by

$$\sigma = 12\pi\alpha \left(\frac{\mu c^2}{E_\gamma}\right) K[2|R^1_{01}|^2 + 4|R^1_{21}|^2 + 3|R^2_{11}|^2 + \tfrac{9}{2}|R^2_{31}|^2] ,$$

where

$$R^J_{l1} = \int R^*_l(Kr)\left[2j_J\left(\frac{M_T}{M}qr\right) + (-)^J j_J\left(\frac{M_\alpha}{M}qr\right)\right] R_{11}(r) r^2 dr ,$$

$$M = M_T + M_\alpha ,$$

and

$$q = E_\gamma/\hbar c .$$

The differential cross section is calculated from

$$\frac{d\sigma}{d\Omega}(90^\circ) = 3\sqrt{4\pi}\,\alpha K\left(\frac{\mu c^2}{E_\gamma}\right)[C_0 - \tfrac{1}{2}C_2 + \tfrac{3}{8}C_4] ,$$

where

$$C_0 = \frac{1}{\sqrt{4\pi}}[2|R^1_{01}|^2 + 4|R^1_{21}|^2 + 3|R^2_{11}|^2 + \tfrac{9}{2}|R^2_{31}|^2] ,$$

$$C_2 = \frac{1}{\sqrt{4\pi}}[4\,\mathrm{Re}(R^1_{01}R^{1*}_{21}) - \tfrac{9}{7}\,\mathrm{Re}(R^2_{11}R^{2*}_{31}) - 2|R^1_{21}|^2 + \tfrac{3}{2}|R^2_{11}|^2 + \tfrac{18}{7}|R^2_{31}|^2] ,$$

$$C_4 = \frac{1}{\sqrt{4\pi}}\frac{18}{7}[4\,\mathrm{Re}(R^2_{11}R^{2*}_{31}) - |R^2_{31}|^2] .$$

Notwithstanding the appearance of Bessel functions in R^J_{l1} our expressions are only valid to the lowest order in q, i.e., $R^J_{l1} \propto q^J$. It should be pointed out that a similar model was used by Czyz.[10] The difference is that Czyz does not invoke the prescription that the ground state should have one node.

The results of this model are shown in Figs. 2 and 5 together with the measured cross sections. $E1$ transitions to the $l=2$ continuum dominate the cross section at these energies. A resonance in the $l=2$ α-^{3}H scattering at $E_K \sim 0.75$ MeV causes the large spike in σ_γ at $E_\gamma \sim 3.25$ MeV. We find that no reasonable adjustment of the strength V_0 for the $l=0$ and $l=2$ continua could give a good fit to the data.

V. CONCLUSION

The α-^{3}H disintegration of ^{7}Li was measured using both real and virtual photons. The photodisintegration measurements gave results that agreed with those extracted from the electrodisintegration data using plane wave virtual-photon theory.

The reaction is characterized by a large bump in the cross section at ≈8 MeV excitation in ^{7}Li having a natural width of ≈7 MeV. There is also slight evidence of another broad resonance centered around 18 MeV which is consistent with the (γ,n) and (n,n) results.[11] The integrated cross section from threshold to 50 MeV is 8.1 MeV mb with 77% of this strength located in the low energy resonance.

A comparison of the data with an α-^{3}H cluster model using a Woods-Saxon potential does not give satisfactory agreement and we must conclude that the data cannot be explained by such a model.

ACKNOWLEDGMENT

We wish to express our thanks to L. O. Dallin for the skillful preparation of the Li foils and the Natural Sciences and Engineering Research Council of Canada for partial financial support.

[1] M. K. Leung *et al.*, Can. J. Phys. 55, 252 (1977).
[2] A. M. Lane, Rev. Mod. Phys. 32, 519 (1960).
[3] N. P. compilation of energy levels. F. Ajzenberg-Selove and T. Lauritsen, Nucl. Phys. A227, 1 (1974).
[4] K. F. Chong *et al.*, Nucl. Phys. A218, 43 (1974).
[5] D. M. Skopik *et al.*, Phys. Rev. C 9, 531 (1974).
[6] J. M. Eisenberg, Phys. Rev. 132, 2243 (1963).
[7] H. W. Koch and J. W. Motz, Rev. Mod. Phys. 31, 920 (1959).
[8] G. M. Griffiths *et al.*, Can. J. Phys. 39, 1397 (1961).
[9] K. Wienhard, private communication.
[10] W. Czyz, Nuovo Cimento 13, 320 (1955).
[11] F. Ajzenberg-Selove, Nucl. Phys. A320, 1 (1979).